



# Deep Water Nutrient Supply for an Offshore *Ulva* sp. Cultivation Project in the Eastern Mediterranean Sea: Experimental Simulation and Modeling

Meiron Zollmann<sup>1</sup> · Hadar Traugott<sup>2</sup> · Alexander Chemodanov<sup>1</sup> · Alexander Liberzon<sup>2</sup> · Alexander Golberg<sup>1</sup>

Published online: 26 August 2019  
© Springer Science+Business Media, LLC, part of Springer Nature 2019

## Abstract

Offshore cultivation of marine macroalgae is a potential sustainable resource for fuel, food, and chemicals. Offshore, the high productivity of macroalgae cultivation depends on external nitrogen supply. The current work examines the idea of supplying nitrogen for *Ulva* sp. cultivation in the oligotrophic Eastern Mediterranean Sea (EMS) by artificial upwelling of nutrient-rich deep seawater (DSW). Growth rates, protein, and starch contents of *Ulva* sp. were measured for time varying fertilizations with nitrate concentrations corresponding to nutrient concentrations of DSW at increasing depths of the EMS. A maximal relative growth rate of 7.4% was measured for fertilizing ten times per week with 5.8  $\mu\text{M}$ , which corresponds to the artificial upwelling from the depth of 700 m at EMS. Protein and starch contents ranged between 1–6 and 8–15% of dry weight. Finally, yields and energetic costs of DSW pumping were modeled for an example case of 10-ha offshore farm. The model predicts a high productivity but low energetic efficiency, which can be improved by coupling the biomass production with offshore power sources such as ocean thermal energy conversion.

**Keywords** Artificial upwelling · Macroalgae · Biorefinery · Offshore cultivation · Eastern Mediterranean Sea

## Introduction

Offshore cultivation of marine macroalgae, also known as seaweed, is a potential sustainable resource for fuel, food, and chemicals [1, 2], which can be co-produced in marine biorefineries [3, 4]. This renewable resource combines a wide array of commodity and high value products [3] with the unique ability to utilize free ocean areas, thus minimizing land and fresh water requirements [1, 5]. In addition, it can provide important environmental services such as pollution mitigation, nutrient recycling, and carbon biosequestration [1, 6, 7].

However, offshore macroalgae production and processing technologies are not mature yet [1, 3]. Multiple challenges,

starting from species choice and controlled cultivation and harvesting solutions [8], through efficient biomass disintegration techniques, to the establishment of cost effective production streams suitable to present global market, are yet to be tackled [3]. Growth rate and chemical composition are key factors for economic production of commodities and other products [7, 9]. For example, in a bioenergy oriented biorefinery, a special emphasis is put on the carbohydrate fraction of the biomass [1], whereas in food oriented biorefinery, the emphasis is put on protein or starch [1, 9]. Protein-to-carbohydrate ratio in macroalgae varies with nutrient availability [10] and, together with growth rate, can serve as useful indicators for nitrogen sufficiency.

Growth rates and chemical composition of macroalgae depend on several main parameters, including light, temperature, salinity, dissolved carbon, and nutrients [9]. Nutrient requirements of macroalgae can be divided into macronutrients, such as nitrogen (N), phosphorus (P), and carbon (C); micronutrients, such as ferrous (Fe), zinc (Zn), and copper (Cu); and vitamins, such as B<sub>12</sub> and thiamine [11]. In marine environments, growth is usually limited by N, P, and Fe [11, 12], and large N supply is a main prerequisite for large scale offshore macroalgae cultivation [9]. Therefore, in many areas, supplying N becomes one of the largest challenges regarding

**Electronic supplementary material** The online version of this article (<https://doi.org/10.1007/s12155-019-10036-3>) contains supplementary material, which is available to authorized users.

✉ Alexander Golberg  
agolberg@tauex.tau.ac.il

<sup>1</sup> Porter School of Environmental and Earth Sciences, Tel Aviv University, Tel Aviv, Israel

<sup>2</sup> School of Mechanical Engineering, Tel Aviv University, Tel Aviv, Israel

offshore biomass production [9]. N supply can be based on synthetic fertilizers, wastewater [4, 13], or N-rich effluents from industrial and agricultural processes, for example, fish cage effluents in the integrated multi-trophic aquaculture (IMTA) [14]. Another fertilization solution, which is less sensitive to the distance from the shore and does not depend on other aquaculture projects, is an artificial upwelling, or pumping of nutrient-rich deep seawater (DSW) to the euphotic zone, and using DSW as fertilizers or directly as a cultivation medium [15, 16].

Artificial upwelling, which is considered a promising geoengineering tool, has been studied during the last few decades, including some nutrient enrichment successful field experiments [17–20]. One interesting artificial upwelling application is the integration of nutrient enrichment and Ocean Thermal Energy Conversion (OTEC) and the utilization of temperature differences between DSW and surface seawater (SSW) as an energy source, which enables to overcome the DSW pumping energetic challenges and even generate excess power [18].

The Eastern Mediterranean Sea (EMS), also known as the Southern Levantine Basin, is an ultra-oligotrophic sea [21], in which artificial upwelling may be an advantageous N source. *Ulva* sp. is a local green macroalgae species in the EMS, characterized by high growth rates and suitability to a broad range of environments [22]. However, previous works have shown that in ambient EMS SSW nutrient concentrations, 3 km offshore, without N addition, daily growth rate (DGR) of *Ulva* is negligible (< 1%) [10].

The goal of this paper is to model potential growth rates of *Ulva* sp. for time varying fertilizations with nitrate concentrations found in different depths of DSW in the EMS, focusing on protein and starch contents. This model, based on results from laboratory *Ulva* sp. cultivation experiments, is subsequently casted into simple upscaling simulations, projecting yields and energetic costs and efficiency of 10-ha *Ulva* sp. cultivation in the EMS, depending on the depth and quantity of pumped DSW. Finally, local bathymetry is examined and presented, casting the evaluated yields into the local geographic context of the Israeli Exclusive Economic Zone (EEZ). The significance of this paper is in assessing the viability of N supply for an offshore *Ulva* sp. cultivation project in the EMS using nitrate concentrations of DSW.

## Methods and Materials

*Ulva* sp. was cultivated in the closed macroalgae photobioreactor system (MPBR) for four consecutive periods of 21 days between January and June 2017, examining the effects of eleven different fertilization scenarios in different seasons. Experiment measurements focused on growth rate and chemical composition, while the environmental

parameters temperature and irradiance were monitored for control. Finally, results were used to simulate the energetic cost and efficiency of large-scale cultivation of *Ulva* sp. in the EMS, if artificial upwelling of DSW from 250, 350, and 700 m is applied as an N source.

## Marine Macroalgae Biomass

Green leafy macroalgae *Ulva* sp. was collected from Haifa during spring 2016 and cultivated in a closed MPBR built for research purposes in the Tel Aviv University (a full description of this MPBR can be found in [23]) (Fig. 1a, b). During cultivation, nutrient concentrations in seawater were maintained at 6.4 mg L<sup>-1</sup> of nitrogen and 0.97 mg L<sup>-1</sup> of phosphorus by fertilizing with ammonium nitrate (NH<sub>4</sub>NO<sub>3</sub>, Haifa Chemicals Ltd., IS) and phosphoric acid (H<sub>3</sub>PO<sub>4</sub>, Haifa Chemicals Ltd., IS). CO<sub>2</sub> was supplied by bubbling air at rates that were periodically adjusted, allowing slow mixing in different biomass densities.

## Experimental Setup

Eleven closed vertical polyethylene photobioreactors were used, welded from 200 μm thick polyethylene sleeve (Polytiv, Israel, length 1 m, width 0.4 m) with embedded anti-UV protection. Each reactor was filled up with 35 L of artificial seawater (ASW, 38–40 ppt, 8.2 pH) composed of distilled water (Zalion Ltd., IS) and 1433.25 g sea salt (Red Sea Ltd.). Assuming half of the surface area was exposed to direct sunlight, the illuminated area of each reactor was calculated as 0.28 m<sup>2</sup> (Fig. 1b). Air bubble mixing was provided from the bottom at a rate of 2 L min<sup>-1</sup> (flowmeter, DFG 6T model, 0.5–8 L min<sup>-1</sup>, Darhor, China). The mixing worked continuously during day time (12 h), while photosynthesis occurs, and for 15 min mixing pulses three times during night time, thus avoiding anoxic conditions. Fresh weight (FW) was determined using an analytical scale (Mettler Toledo, PB-S model, Switzerland, 0.01 g precision) after removing surface water using an electric centrifuge (Spin Dryer, CE-88, Beswin). System error was evaluated in the [Supplementary Data](#).

Four successful runs were performed between January and June 2017. Each run commenced with an acclimation period, in which 200 g FW of *Ulva* sp. from the MPBR was cultivated for 6 to 8 days under ambient conditions in a closed photobioreactor filled up with 35 L ASW without added nutrients. ASW baseline nutrient concentrations were 1.35, 1.89, 2.35, 0.09, and 0.19 μM for silicate, ammonium, nitrate, nitrite, and phosphate, respectively (Segmented Flow Analysis, NIOZ-Yerseke, the Netherlands). We performed the acclimation to minimize effects of environmental changes and of nutritional history on growth rates and chemical composition [11].

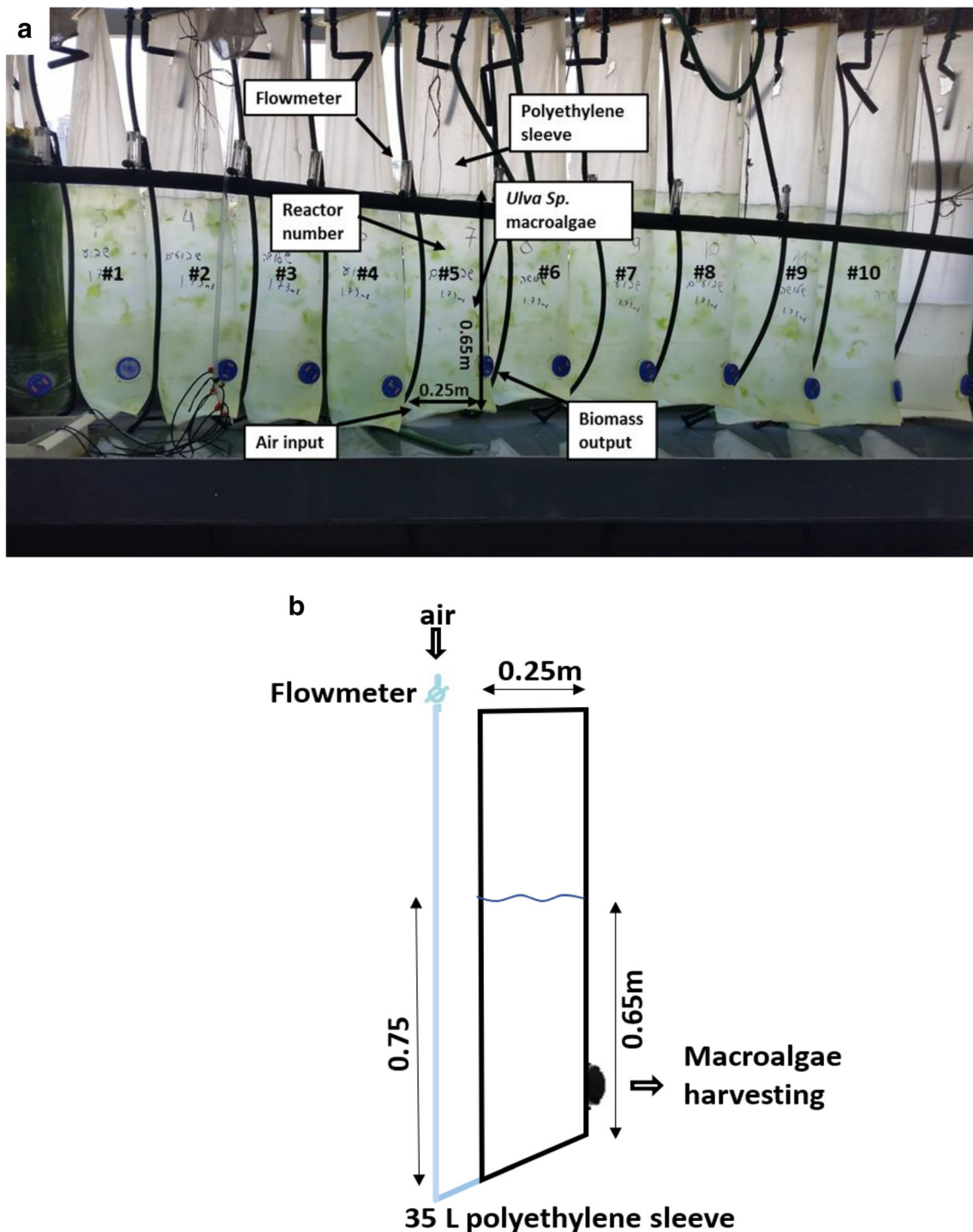


**Fig. 1** a Illustration of the 11 reactors’ MPBR system during a cultivation experiment. b A front view sketch of a single MPBR reactor

Next, ten batches of 10 g FW were weighed and cultivated for 21 days in ten similar reactors, filled up with new ASW. During the cultivation period, the reactors were fertilized as described in “Fertilization.” Finally, after 21 days, biomass samples were harvested; weighed (FW); dried in 40 °C; grinded using liquid nitrogen,

mortar, and pestle; and then kept at 4 °C until analysis. In returns 3 and 4, the different reactors were harvested after 6, 13, and 21 days, thus examining growth rate changes with time, allowing to differentiate between effects of the nutritional history and the fertilization applied during the experiment.

## Fertilization

Twelve different combinations of three nitrate concentrations (2, 3.5, and 5.8  $\mu\text{M}$ ) and five fertilizing frequencies (1, 2, 3, 5, and 10 times per week) ( $N=27$ ) were examined (Table 1). Nitrate concentrations were chosen based on winter measured values in the depths of 250, 350, and 700 m offshore the EMS ( $33^\circ 30' \text{N}$ ,  $29^\circ 30' \text{E}$ ), as reported by [21]. Each fertilization event simulated the addition of a nitrate quantity equivalent to the nitrate in 35 L of DSW from a specific depth. Focusing solely on N effects, P was added in a molar ratio of 16:1 N:P, thus preventing P limitation [11].

Fertilization was performed using a stock solution prepared by dissolving 10 g  $\text{NaNO}_3$  (Merck, Germany) and 0.882 g  $\text{NaH}_2\text{PO}_4$  (CalBiochem, CA) into 1 L of ultra-pure water. Stock solution was filtered through 0.22- $\mu\text{m}$  disposable filters and kept in 4  $^\circ\text{C}$  in a glass autoclaved bottle. The control reactor fertilization concentration was chosen to ensure excess N and P throughout the whole experiment [24–26], striving to achieve maximal growth rates for the specific conditions of each run.

Fertilization efficiency of the different treatments was examined by calculating how much biomass was produced per added N.

## Temperature and Irradiance

Data regarding ambient temperature and irradiance during the experiment period was extracted from the IMS data base from the Israel Meteorological Services (<http://www.ims.gov.il/IMS/CLIMATE/LongTermRadiation/>). Ambient temperature ( $^\circ\text{C}$ ) data was based on the Tel Aviv coastal measurement station, which provides information in a 3-h resolution. Solar irradiance data was based on the Beit Dagan measurement station, which provides information about accumulated global irradiance with 1 h resolution. The irradiance data was multiplied by a factor of 0.1 which best reflects the shading effect in the MPBR [23]. In the current work, hourly solar irradiance power per square

meter was summed to produce daily solar irradiance energy per square meter. In addition, water temperature was measured during February and May–June 2017 by an Onset® HOBO® sensor UA-002-08 (Onset Inc. MA).

## Growth Rate

Relative growth rate (RGR) was calculated by Eq. (1), as used previously [27–29].

$$\text{RGR} = 100\% \frac{\ln(\text{FW}_{\text{out}}/\text{FW}_{\text{in}})}{N_{\text{days}}} \quad (1)$$

where  $\text{FW}_{\text{in}}$  (g) is the initial fresh weight,  $\text{FW}_{\text{out}}$  (g) is the final fresh weight, and  $N_{\text{days}}$  is the number of cultivation days under specific fertilizing conditions.

## Protein Quantification

Protein was extracted using the following protocol: (1) 15 mg of dry algae powder were weighed into 2-mL capped tubes (Benchmark Scientific (NJ, USA)), next filled up (to the third) with beads (zirconia, 2 mm, Sarstedt) and 1.5 mL 2 M NaOH; (2) three sessions of beating (60 s, 4800 rpm) in a bead beater (Biospec (Ok, USA)) followed by cooling (a few minutes in air temperature) were performed; (3) tubes were centrifuged (Eppendorf microcentrifuge 5424, Sigma-Aldrich, USA) for 20 min in 14,680 rpm and supernatant was kept in  $-20^\circ\text{C}$ ; (4) finally, supernatant was defrosted in room temperature, diluted (1:20), and used for the protein quantification.

Protein content was determined by a modified version of Lowry method [30] using bovine serum albumin (BSA) as protein standard, as recommended by a previous study that evaluated the different extraction and quantification methods of protein for marine macro- and microalgae [31]. Briefly, using a 96-well plate, 100  $\mu\text{L}$  of either diluted samples or diluted standard solutions was added, followed by 200  $\mu\text{L}$  of biuret reagent (a mixture of 0.5 mL of 1% cupric sulfate with 0.5 mL of 2% sodium potassium tartrate and 50 mL of 2%

**Table 1** Fertilizing concentrations and frequencies

Reactor no.		1	2	3	4	5	6	7	8	9	10	
Runs 1 and 2 (30/1-20/2, 20/2-13/3)	Simulated depth (m)	250			350			700			Control	
	$\text{NO}_3^-$ ( $\mu\text{M}$ )	2	2	2	3.5	3.5	3.5	5.8	5.8	5.8	430	
	Fertilizing frequency ( $\text{week}^{-1}$ )	1	2	3	1	2	3	1	2	3	1	
Run 3 (22/5-12/6)	Simulated depth (m)			700			700			700		Control
	$\text{NO}_3^-$ ( $\mu\text{M}$ )			5.8			5.8			5.8		430
	Fertilizing frequency ( $\text{week}^{-1}$ )			10			10			10		1
Run 4 (5/6-26/6)	Simulated depth (m)				700				700		Control	
	$\text{NO}_3^-$ ( $\mu\text{M}$ )				5.8				5.8		430	
	Fertilizing frequency ( $\text{week}^{-1}$ )				5				5		1	

sodium carbonate in 0.1 N NaOH). After extensive mixing by pipetting, the plate was incubated at room temperature for 10–15 min. Next, 20 μL of Folin and Ciocalteu’s reagent (Sigma-Aldrich, USA) diluted twice (final concentration of 1 N) was added and mixed by pipetting. Finally, the plate was incubated at room temperature for 30 min before reading the absorbance at 650 nm using a Tecan spectrophotometer (Infinite 200 Pro, Tecan, Switzerland).

### Starch Quantification

Starch content was determined using an enzymatic based total starch assay kit (K-TSTA-100A, Megazyme, Ireland), applied on 10 mg dry algae powder in 1.5-mL tubes. Both protein and starch analyses were based on triplicate extractions and triplicate colorimetric measurements.

### Elemental Analysis

Elemental analysis was performed on representative group of samples ( $N = 14$ ) at the Technion, Chemical, and Surface Analysis Laboratory, using Thermo Scientific CHNS Analyzer (Flash2000).

### Dry Matter and Ash Quantification

Ash content was measured for a representative group of samples ( $N = 8$ ). Dry algae powder ( $0.5 \pm 0.1$  g) was weighted ( $m_1 =$  mass of sample + crucible) and then dried at 105 °C using the conventional oven for 24 h in preweighted clean crucibles ( $m_2 =$  crucible mass). The crucibles were cooled down in a desiccator, weighted ( $m_3$ ), and ignited at 500 °C for 3 h in a muffle furnace (M.G. Furnaces, India) and then cooled down to 105 °C. The crucibles were finally removed from the furnace, kept in a desiccator to cool them down at room temperature, and weighted ( $m_4$ ). Dry matter and ash content were calculated as shown in Eq. (2) and Eq. (3).

$$\text{Dry matter content (\%)} = \frac{m_3 - m_2}{m_1 - m_2} \tag{2}$$

$$\text{Ash content (\% of dry matter)} = \frac{m_4 - m_2}{m_3 - m_2} \tag{3}$$

Results of chemical composition analyses were adjusted to percent of DW by dividing the results in the average dry matter content.

### Estimation of Offshore Production Potential at the EMS

Biomass yields, production of protein, and production of starch for each scenario were extrapolated to an area of 10 ha using Eq. (4) and Eq. (5). Constant amounts of N and

irradiance per initial biomass weight were kept by changing the dimensions of the base, reactor size, and cultivation unit. Therefore, the reactor shading factor of 0.1 was simulated by decreasing the equivalent offshore illuminated area to 0.028 m<sup>2</sup>, while keeping the 35 L volume by increasing the depth to 1.25 m. Light extinction in the water was neglected. An alternative extrapolation assumed a lower, 5-fold, irradiance difference between offshore and the MPBR. Thus, an offshore illuminated area of 0.056 m<sup>2</sup> was used, followed by a cultivation depth of 0.625 m. We called the first extrapolation high irradiance extrapolation (HIE) and the second low irradiance extrapolation (LIE). The illuminated area is a suitable conversion factor as it reflects both the global irradiance, which is useful for energy balance studies [32], and the photosynthetic available radiation (PAR), which can be used to calculate photosynthesis efficiency [33, 34].

$$Y_{10 \text{ hectare, FW}} = \frac{Y_{R, FW}}{a_R^*} \frac{10^5 \text{ m}^2}{10 \text{ hectare}} \frac{\text{ton FW}}{10^6 \text{ g FW}} \tag{4}$$

where  $Y_{10 \text{ hectare, FW}}$  (ton FW 10 ha<sup>-1</sup> 21 days<sup>-1</sup>) and  $Y_{R, FW}$  (g FW m<sup>-2</sup> 21 days<sup>-1</sup>) are the expected biomass yields in an area of 10 ha and the measured yield in the reactor, both during 21 days of cultivation;  $a_R^*$  is the equivalent offshore illuminated area, 0.028 m<sup>2</sup> or 0.056 m<sup>2</sup>; and  $\left(\frac{10^5 \text{ m}^2}{10 \text{ hectare}}\right)$  and  $\left(\frac{\text{ton FW}}{10^6 \text{ g FW}}\right)$  are constants used for unit conversion.

$$Y_{10 \text{ hectare, protein/starch}} = Y_{10 \text{ hectare, FW DW}} : \text{FW pr/st cont} \frac{\text{kg DW}}{\text{ton DW}} \tag{5}$$

where  $Y_{10 \text{ hectare, protein/starch}}$  (kg protein/starch 10 ha<sup>-1</sup> 21 days<sup>-1</sup>) is the expected production of protein or starch in an area of 10 ha during 21 days of cultivation;  $Y_{10 \text{ hectare, FW}}$  (ton FW 10 ha<sup>-1</sup> 21 days<sup>-1</sup>) is the expected biomass yield; DW : FW is the dry to fresh weight ratio, which was defined as 0.15 based on previous works [32]; and pr/st cont is the protein or starch content (kg protein/starch ton DW<sup>-1</sup>), which were measured as described in “Protein quantification” and “Starch quantification.”

### Energetic Requirements of Artificial Upwelling

First, DSW flow was calculated by extrapolating the simulated water exchange from the laboratory experiment to an area of 10 ha, using Eq. (6).

$$Q_{10 \text{ hectare, scenario 1}} = \frac{Q_{R, \text{scenario 1}}}{a_R^*} \frac{\text{week}}{604,800 \text{ s}} \frac{10^5 \text{ m}^2}{10 \text{ hectare}} \tag{6}$$

where  $Q_{10 \text{ hectare, scenario 1}}$  (m<sup>3</sup> s<sup>-1</sup>) is the DSW flow in an area of 10 ha;  $Q_{R, \text{scenario 1}}$  (m<sup>3</sup> week<sup>-1</sup>) is equal to 0.035 m<sup>3</sup>, the volume of the reactor which is simulated to be replaced once a

week;  $a_R^*$  is the equivalent offshore illuminated area,  $0.028 \text{ m}^2$  or  $0.056 \text{ m}^2$ ; and  $\left(\frac{10^5 \text{ m}^2}{10 \text{ hectare}}\right)$  and  $\left(\frac{\text{week}}{604,800 \text{ s}}\right)$  are constants used for unit conversion. For simplicity, increased fertilization frequencies were expressed by additional pumps and pipes, thus performing all calculations on one effective flow.

Next, pumping power and energy requirements were calculated using the Darcy-Weisbach Eq. (7) to calculate head losses and Eq. (8) to calculate the hydraulic power.

$$H_L = f \left( \frac{L}{D} \right) \left( \frac{v^2}{2g} \right) \quad (7)$$

where  $H_L$  is the total head loss (m),  $f$  is the friction factor,  $L$  is the length of the pipe,  $D$  is the diameter of the pipe, and  $v$  is the average liquid velocity in the pipe.  $L$  was determined according to the depth of the source water (250, 350 or 700 m).  $D$  was chosen to be 0.5 m based on a comparison of energy requirements and losses at different diameters (see “Specific Energetic Requirements”; Table 2).  $v$  was calculated to be 0.5 or  $1.1 \text{ m s}^{-1}$  for the smallest flow (depending on the extrapolation method) and was kept constant by adding pipes, as done for the flow.  $f$  was determined to be 0.014 or 0.016 according to the moody diagram (assuming a PVC pipe and roughness of  $3.334 \text{ } \mu\text{m}$  [35]).

$$P_h = \rho g Q H \quad (8)$$

where  $P_h$  is the hydraulic power of the pump (W),  $\rho$  is a representative DSW density ( $1027 \text{ kg m}^{-3}$ ),  $g$  is the universal gravitation constant ( $9.81 \text{ m s}^{-2}$ ),  $Q$  is the volumetric flow of DSW through the pump ( $\text{m}^3 \text{ s}^{-1}$ ) calculated by Eq. (4), and  $H$  is the head difference across the pump (m) and was determined as the sum of the hydrostatic component, equivalent to the pumping depth and the head losses calculated above.

Based on the chosen pipe dimensions, energy consumption per 21 days per 10 ha was calculated for the different fertilization scenarios by Eq. (9).

$$E_{\text{nutrients}} = \frac{P_h}{\eta} N_{\text{days}} N_{\text{pumps}} 24 \left( \frac{\text{hours}}{\text{days}} \right) 0.001 \left( \frac{\text{MWh}}{\text{kWh}} \right) \quad (9)$$

**Table 2** Energy requirements and losses (in brackets) [MJ] for pumping  $1 \text{ m}^3$  of DSW from different depths in a flow rate of  $1 \text{ m}^3 \text{ s}^{-1}$ , using different diameters

Depth (m)	250	350	700
D (m)			
0.4	3.23 (0.26)	4.52 (0.37)	9.03 (0.74)
0.5	3.05 (0.09)	4.27 (0.12)	8.54 (0.24)
0.6	3.00 (0.03)	4.20 (0.05)	8.39 (0.10)
1	2.97 (0.01)	4.15 (0.01)	8.31 (0.03)

where  $E_{\text{nutrients}}$  is the energy consumption (MWh);  $P_h$  the hydraulic power of the pump (kW);  $\eta$  is the pumping efficiency, assumed to be 0.85;  $N_{\text{days}}$  is the number of cultivation days;  $N_{\text{pumps}}$  is the number of pipes or pumps, which is equivalent to the fertilizing frequency; and  $24 \left( \frac{\text{hours}}{\text{days}} \right)$  and  $0.001 \left( \frac{\text{MWh}}{\text{kWh}} \right)$  are constants used for unit conversion.

## Energetic Efficiency of Artificial Upwelling

Energetic efficiency of the artificial upwelling was examined by the Exergy Return On Investment (ExROI) indicator, as suggested by [32]. This indicator relates only to fossil fuel derived exergy streams. In its most simplified form, ignoring exergy streams related to labor, capital, waste, and ecosystem services, and assuming no mixing will be needed in offshore cultivation, it can be calculated using Eq. (10).

$$\text{ExROI} = \frac{E_{\text{produced biomass}}}{E_{\text{nutrients}}} \quad (10)$$

where ExROI is the dimensionless energetic performance efficiency indicator,  $E_{\text{produced biomass}}$  is the energetic value of the produced biomass (MWh), calculated as described in [32], and  $E_{\text{nutrients}}$  is the pumping energetic cost (MWh), both for 21 days cultivation in 10 ha.

## Ocean Thermal Energy Conversion

OTEC can be integrated with the DSW pumping and serve as a power source for the fertilization task [18]. The maximum theoretical efficiency for full utilization of this resource is calculated by Eq. (11), and its maximum available energy is calculated by Eq. (12).

$$\eta_{\text{max}} = \frac{1}{2} \left( \frac{T_h}{T_c} - 1 \right) \quad (11)$$

$$W_{\text{max}}/\text{m}^3 = k (T_h - T_c) \eta_{\text{max}} \quad (12)$$

where  $\eta_{\text{max}}$  is the maximal theoretical efficiency of a heat engine,  $T_h$  and  $T_c$  are the temperatures of SSW and DSW in  $^{\circ}\text{K}$  units,  $W_{\text{max}}$  is the maximum available energy in units of  $\text{J m}^{-3}$ , and  $k$  is the specific heat of water,  $4.187 \times 10^6 \text{ J } ^{\circ}\text{K}^{-1} \text{ m}^{-3}$ .

## Data Analysis

HSD Tukey mean comparisons were used to compare the effect of the different fertilization treatments on growth rates. Spearman’s test was used to compare the results of runs 1 and 2, in which the same fertilization treatments were applied. Statistical analysis was performed using JMP pro 14 (SAS Institute Inc, NC, USA) and Microsoft Excel (2016).

## Results and Discussion

### Growth Rates

RGR was measured for different combinations of fertilizing concentrations (2, 3.5, and 5.8  $\mu\text{M NO}_3^-$ ) and frequencies (1, 2, 3, 5, and 10 pulses per week) (Fig. 2a). RGR values of the control reactors, representing *Ulva* sp. cultivated year-round in excess nutrients in an MPBR located in Tel Aviv, Israel, ranged between 7 and 10.5%  $\text{day}^{-1}$ , with an average RGR of 9.1%  $\text{day}^{-1}$  along 21 days. In comparison, RGR of *Ulva* sp., fertilized to EMS DSW nitrate concentrations, varied between negligible growth ( $< 1\% \text{ day}^{-1}$ ) for the lowest nutrient additions and a maximum of 6.3–7.4%  $\text{day}^{-1}$  for the highest nutrient addition (5.8  $\mu\text{M}$ , 10  $\text{week}^{-1}$ ). When examining separately only the fertilization frequencies of 1, 2, and 3  $\text{week}^{-1}$  by HSD Tukey mean comparisons, no difference in RGR was found between any combination of frequency and fertilization concentration ( $P$  value  $> 0.05$ ). Although the differences between those treatments were insignificant, they did follow a similar trend (Spearman's  $r = 0.88$ ). However, the combination of 5.8  $\mu\text{M}$  with 10  $\text{week}^{-1}$  and the control achieved higher RGRs ( $P$  value  $< 0.03$  and  $P$  value  $< 0.0001$ ). The control RGR was higher also than that of the combination of 5.8  $\mu\text{M}$  with 5  $\text{week}^{-1}$  ( $P$  value  $< 0.01$ ).

For the sake of comparing different nutrient enrichment treatments (i.e., different combinations of fertilization concentrations and frequencies), we defined the term normalized N

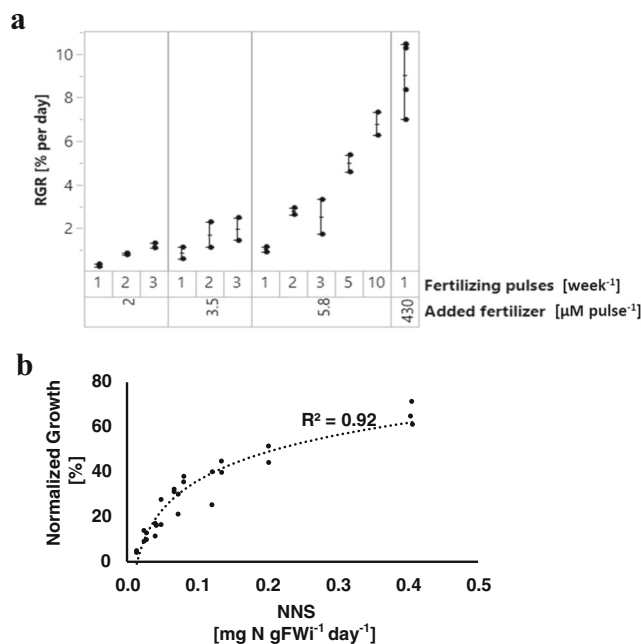


**Fig. 2** a Relative growth rates for different combinations of fertilizing concentrations and frequencies. b Normalized growth (RGR/control RGR) rate vs normalized N supply (mg added N per g FW initial biomass per day)

supply (NNS), which is the total N that was added to the system, normalized per fresh weight of initial biomass per day. This term relates not only to the concentration but also to the biomass density, volume of water, fertilization frequency, and cultivation duration and, therefore, can better describe the effective amount of N added to the system.

Another useful term we used is normalized growth, which is the RGR of a reactor normalized to the RGR of its control reactor. By normalizing to the control, time related external effects, such as the effect of light and temperature, are eliminated, and fertilization effect is more noticeable. When examining the effect of NNS on normalized growth, a direct logarithmic correlation ( $R^2 = 0.92$ ) is evident (Fig. 2b). The maximal normalized growth rates, 61–71.5%, were achieved for the combination of 5.8  $\mu\text{M}$  nitrate and 10  $\text{week}^{-1}$  frequency. These values were achieved with an NNS 7.5 times lower than the NNS of the control, suggesting 2.5–3.5 times higher fertilizing efficiency, in terms of gram produced biomass per gram of added N. In similar experiments ( $N = 6$ ), performed between July and October 2017, growth rates were measured for the same NNS, applied this time by adding 58  $\mu\text{M}$  once a week. The results of these experiments, RGR of 3–6%  $\text{day}^{-1}$  (compared to 5–8.5%  $\text{day}^{-1}$  of the control), normalized growth rates of 36–83%, and fertilization efficiencies 1.4–5.6 higher than the control, are slightly lower, which may be explained by different temporal distributions and by seasonal effects.

Changes of RGR with cultivation duration in the 5.8  $\mu\text{M}$ , 10  $\text{week}^{-1}$ , and 5  $\text{week}^{-1}$  nutrient treatments are presented in Fig. 3. Although NNS in the 10  $\text{week}^{-1}$  was double than in the 5  $\text{week}^{-1}$ , a clear difference in RGR ( $P$  value  $< 0.05$ ) was observed only after 3 weeks. Our proposed explanation is that in the first period of cultivation, growth is primarily affected by the state of the internal nutrients, which result from the nutritional history. Furthermore, these results show that 21 days were a long enough cultivation period to examine fertilization effects, regardless of the varying initial tissue N conditions. In addition, the analysis presented in the

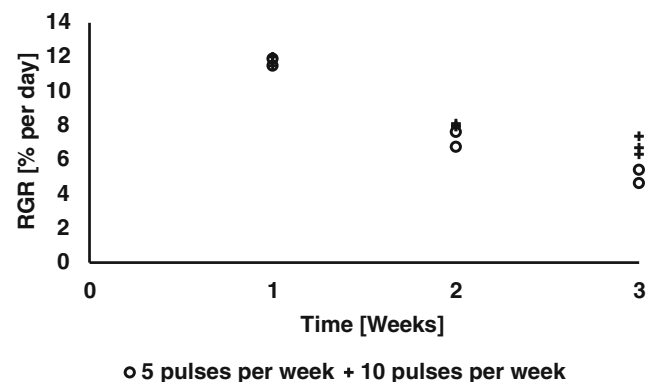


**Fig. 3** Relative growth rate vs time in the reactors fertilized by 5.8  $\mu\text{M NO}_3^-$  and 5 or 10  $\text{week}^{-1}$

**Supplementary Data** confirms that all results and identified trends presented above (i.e., RGR differences) are not affected by the system setup. Therefore, RGR differences within each run, or alternatively, normalized growth rate differences in all runs, are due to fertilization treatment alone. However, the effect of “date” related factors, such as temperature and irradiance, is significant and therefore is further analyzed and discussed (see “**Temperature and Irradiance Effects**”).

## Chemical Composition

Protein and starch were used to evaluate the changes in the chemical composition of the produced biomass. As expected from previous works [10, 36, 37], protein was high (14–21% of DW) and starch was low (2–3% of DW) in all control reactors, besides one control reactor with an unexplained starch result (8% of DW). When focusing on the reactors fertilized to DSW nitrate concentrations (Fig. 4a), no change in protein with NNS was identified ( $P$  value  $> 0.05$ ), and most measurements were in the range of 4–6% of DW. This constancy can be explained by the term critical tissue N content, which was introduced by [38] and further discussed by [11]. This term means that when the macroalgae’s tissue N level drops below a certain level, its growth slows down. Consequently, the decrease in tissue N slows down too until tissue N (and protein) stabilizes. These results indicate that in all treatments, except the control, growth was limited by N availability. Nevertheless, changes of growth rate with NNS can be explained by different equilibriums that were achieved

between N consumption via growth and N uptake. N to protein conversion factor was calculated to be 5.64 (Fig. 4b), compared to a green macroalgae average of 5.13 ratio [39].

Starch, on the contrary, was not constant and increased in the lowest NNS from about 9% up to 15% of DW. Starch serves as the main reserve carbohydrate in *Ulva* sp. and is accumulated in nutrient stress conditions, when N limitations decrease the production of new biomass [37]. Furthermore, previous works have found an inverse correlation between starch and growth rate and between starch and tissue N [37]. A linear inverse correlation between starch and tissue N was found also here (Fig. 4b;  $R^2 = 0.77$ ). Considering the significant increase in starch content under severe nutrient stress, a previous work suggested applying a two-step cultivation: first, a nutrient-rich step for high biomass production, and second, a nutrient-limited phase for the carbohydrate/starch accumulation phase [10].

## Temperature and Irradiance Effects

Variation of ambient temperature and daily irradiance at the MPBR surface along the cultivation periods is presented in Fig. 5a. Water temperature, when measured, followed the same trend and same range as air temperature. Effects of temperature and irradiance were analyzed by plotting growth rates and protein and starch content of the control reactors vs average temperature and daily irradiance ( $N = 4$ ), thus eliminating the effect of the nutrients (Fig. 5b, c). Control RGR has increased linearly with ambient temperature ( $R^2 = 0.70$ ) and

**Fig. 4** Protein and starch content (% of DW) vs **a** NNS (mg added N per g of initial fresh weight per 21 days) and **b** N content (% of DW)

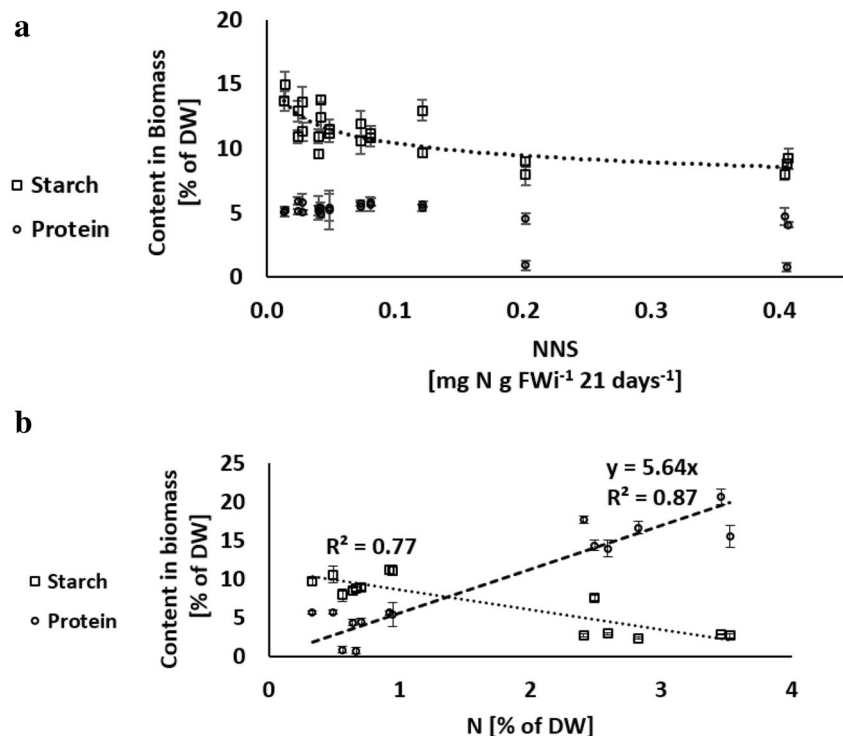
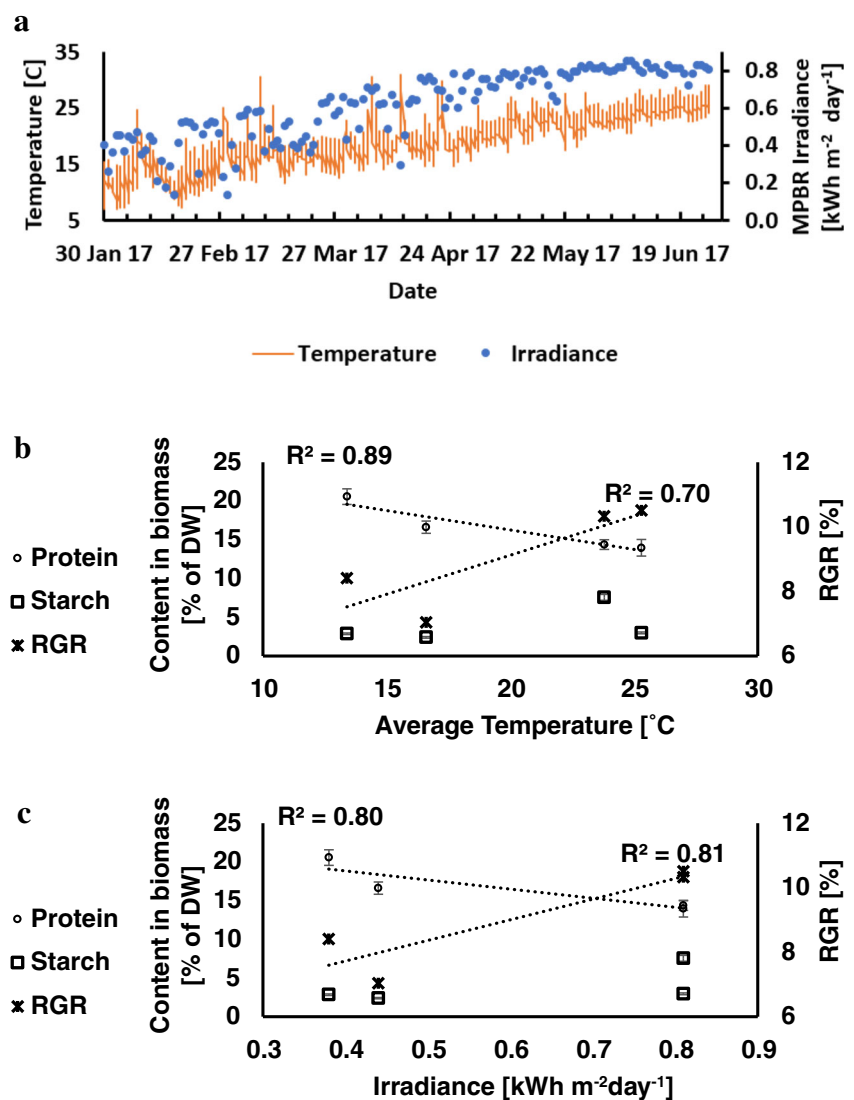


**Fig. 5** Variation of ambient temperature and MPBR daily global solar irradiance energy per square meter with time (a) and of RGR and starch and protein content (% of DW) in control reactors with daily average temperature (b) and irradiance (c)



irradiance ( $R^2 = 0.81$ ). However, this trend may apply only for a specific temperature range. For example, a previous work found that at average, temperatures higher than 27 °C and productivity of this *Ulva* sp. may decrease [32]. Inversely to the RGR, protein content decreased linearly as irradiance increased ( $R^2 = 0.80$ ), a phenomenon identified previously as light limited growth [37]. Low levels of starch also reflected a light-limited growth, as starch tends to accumulate under N limitation rather than under light limitation [37].

**Offshore Cultivation Simulation**

The cultivation experiments presented in previous sections were designed to examine growth rates and chemical compositions of *Ulva* sp. cultivated under N supply that simulate different artificial upwelling scenarios in the EMS. In this section, we project the production of dry biomass, protein and starch, and the energetic cost and efficiency to a large-

scale cultivation of *Ulva* sp. in the EMS, pumping DSW from 250, 350, and 700 m as a N source. This projection is based on a preliminary calculation of specific energetic cost of DSW pumping and on extrapolating both yields and energetic costs to an area of 10 ha and the respective DSW flows. The implications of this projection are later discussed, emphasizing the importance of the power source to the energetic viability of this project.

**Specific Energetic Requirements**

Energy is a main operation input in any artificial upwelling project and has a crucial effect on its feasibility. A previous work, which focused specifically on airlift artificial upwelling [19], pointed the diameter as the most significant geometric parameter of the upwelling pipe efficiency. After examining diameters of 0.4, 1, and 2 m and discussing how increasing diameters are an energetic advantage but a construction and

maintenance disadvantage, the conclusion of [19] was that a mid-range diameter would best fit. Here, we started with calculating energy requirements and losses for pumping  $1 \text{ m}^3$  in four different diameters (0.4, 0.5, 0.6, and 1 m) and the three examined depths (Table 2) in a flow rate of  $1 \text{ m}^3 \text{ s}^{-1}$ . A comparison between energy requirements (and losses) shows a sharp decrease when enlarging the diameter from 0.4 to 0.5 m, followed by milder decreases when further enlarging the diameter. Based on these results, and after ensuring DSW velocity is reasonable, we chose the diameter of 0.5 m, in which we further conducted the full energetic analysis.

### Offshore *Ulva* sp. Production—Energy and Productivity

Offshore biomass production can be utilized to produce a wide variety of products, for example, via the co-production or biorefinery concept [3, 4]. Here, we focused on dry biomass, protein, and starch, attempting to evaluate the energetic cost of performing artificial upwelling for their production in the EMS. The projection of the results to 21 cultivation days in an area of 10 ha offered the production of 0.4–17.1 ton of dry biomass, including 21–751 kg protein and 59–1484 kg starch, in an energetic cost of 309–8656 MWh (HIE), or 0.2–8.6 ton of dry biomass, including 11–375 kg protein and 30–742 kg starch, in an energetic cost of 154–4323 MWh (LIE), depending on the fertilization scheme. Figure 6a presents the projected production potentials, following the HIE, as a function of invested energy. A linear correlation was found between increased energy input, equivalent to increased fertilization, and the increase in dry biomass ( $R^2 = 0.98$ ), protein ( $R^2 = 0.96$ ), and starch ( $R^2 = 0.96$ ). Figure 6b relates to the energy input as singular fertilization scenarios, combining pumping depth and number of pumps per 10 ha, and presents the productivity and energetic cost of protein and starch production in each scenario. These energetic costs are equivalent to 0.35–0.74 MWh per kg of dry biomass or, when focusing on specific products, 6.5–14.5 MWh per kg of protein and 3.1–6.1 per kg of starch. The energetic cost of specific products can be reduced by applying co-production, thus allowing better utilization of the produced biomass.

A comparison of *Ulva* sp. protein yields and ExROI to those of terrestrial and marine crops is presented in Table 3. The marine crop comparison relates to results from *diatoms* artificial upwelling-based cultivation experiments, conducted in the 1970s in the St. Croix (U.S. Virgin Islands). In these experiments, three 7.5-cm-diameter polyethylene pipelines pumped DSW from a depth of 870 m into two pools, in which *Diatoms* were cultivated, serving later as shellfish feed. The combined nitrate and nitrite concentration of these DSW was  $2.4 \mu\text{M}$  [18]. This comparison suggests that in a year-round cultivation, applying the scenario 11 fertilization treatment, *Ulva* sp. farming can yield 0.6–1.2 ton protein per hectare, more than any terrestrial crop [40], but less than the *diatoms*

artificial upwelling-based cultivation experiments [18]. *Ulva* sp. protein yield inferiority compared to diatoms may be explained primarily by large differences in biomass protein content (4.4% vs 58%). However, this comparison is limited due to different experimental setups, relating, for example, to the cultivation system dimensions, cultivated species, and environmental conditions. In addition, it should be noted that extrapolating to a yearly yield ignores seasonal changes in environmental conditions such as irradiance and temperature.

Starch, when co-produced with protein, is projected to yield 1.2–2.3 ton per hectare annually. In comparison, corn, which is farmed in North America as a starch source too, can yield annually up to 7.2 ton of dry corn [41] and 4.3–4.7 ton starch [42] per hectare, 1.9–3.9 times more than the *Ulva* sp. projected yield.

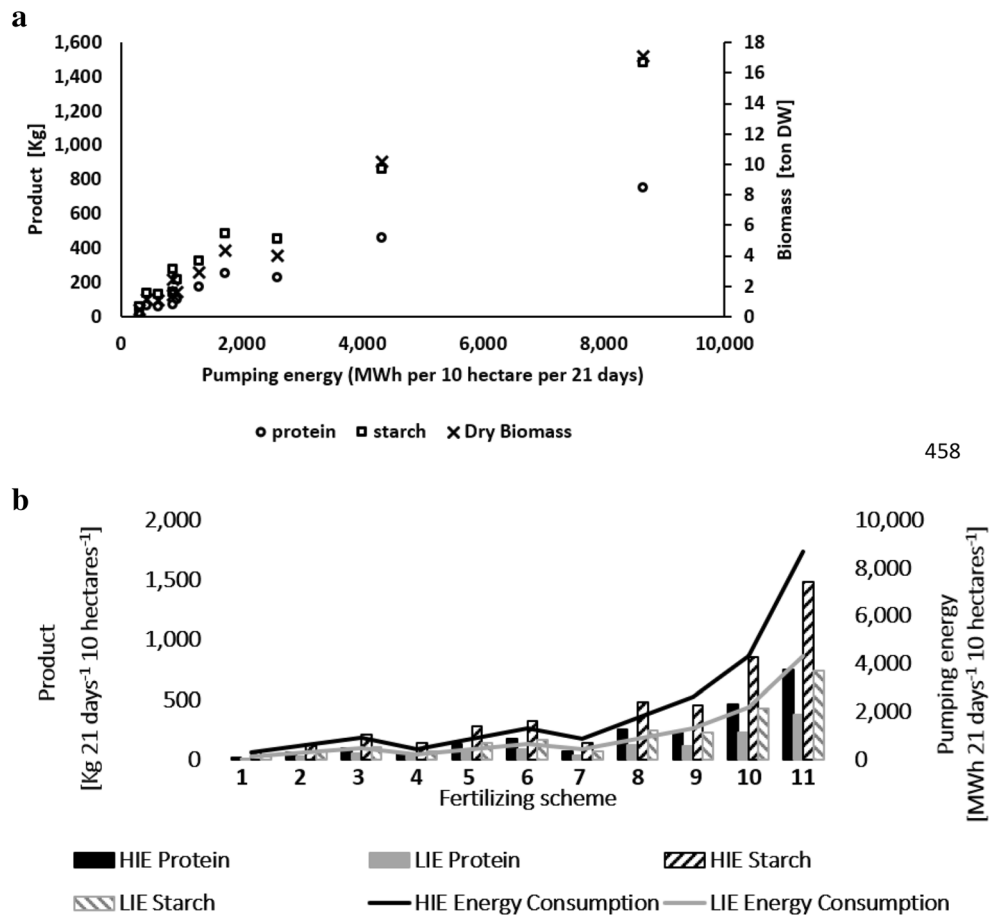
ExROI of artificial upwelling-based *Ulva* sp. cultivation in the EMS is projected to be in the range of 0.0037–0.0078. This indicates a very low energetic efficiency in comparison to other crops (Table 3). However, as the *Ulva* sp. protein and starch productivity may be competitive, means of improving the energetic performance should be further discussed (see “Offshore Power Supply”).

### Offshore Power Supply

DSW pumping requires high-energy inputs and a suitable power supply. In case of a fossil fuel-based power supply, the energetic efficiency of the examined EMS project is expected to be very low (see “Offshore *Ulva* sp. Production—Energy and Productivity”). Using a threshold of positive ExROI, maximal allowed pumping power for the different fertilization scenarios following the HIE was calculated (Table 4). These values may be relevant only in cases of high nitrate concentrations and shallow depths, as found, for example, in the Norwegian fjords [43].

Alternatively, self-powered artificial upwelling systems such as wave pumps can help overcome this energetic inferiority [16, 17]. A theoretical work on this topic estimated that in the condition of 1.90 m wave height and 12 s wave periods, a wave pump can produce a flow rate in the range 0.45 to  $0.95 \text{ m}^3 \text{ s}^{-1}$  [44]. However, in a field experiment, which suffered from a complete material failure after a few hours, the measured flows were an order of a magnitude lower [45]. A more advanced solution, which is progressing these days towards the construction of field demonstration plants, is the distributed generation (DG) method, combining units of wind turbines, wave energy converters, photovoltaic arrays, and a diesel generator, powering together an air compressor for airlift pumping [17]. Airlift pumps, which were recently proposed as candidates for upwelling applications due to their simplicity and lack of moving mechanical parts, are still in developmental stages. The development of self-sufficient power supply techniques, such as the DG, may be an

**Fig. 6 a** Production of dry biomass, protein, and starch as a function of energy invested in pumping of DSW for fertilization, according to the HIE (**b**). Production of protein and starch and energy consumption of the different artificial upwelling fertilization schemes in both LIE and HIE: 1 250 m, 1 pump; 2 250 m, 2 pumps; 3 250 m, 3 pumps; 4 350 m, 1 pump; 5 350 m, 2 pumps; 6 350 m, 3 pumps; 7 700 m, 1 pump; 8 700 m, 2 pumps; 9 700 m, 3 pumps; 10 700 m, 5 pumps; 11 700 m, 10 pumps; both during 21 days of cultivation in an area of 10 ha



458

important progress towards the implementation of airlift pumps [19].

Furthermore, some designs propose to utilize salt and temperature gradients (perpetual salt fountain) and even produce power (OTEC) while pumping DSW [16, 17]. However, both technologies are limited to specific geographical zones. The perpetual salt fountain cannot work where the salinity of the SSW is higher than that of the DSW [17]. Similarly, the OTEC requires a minimum temperature difference of 10 °C (and preferably more than 20 °C) between SSW and DSW.

Applying OTEC in the EMS may be relevant only in summer conditions (26 °C in the surface and 13.5 °C in the depth [21]). In these conditions, the maximal power generation efficiency is 2.2% and the maximal available energy is 1.14 MJ m<sup>-3</sup>. In comparison, in the conditions of the U.S. Virgin Islands (27 °C in the surface and 7 °C in the depth), the maximal power generation efficiency is 3.6% and the maximal available energy is 2.91 MJ m<sup>-3</sup> [18]. Therefore, the pumping cost in a 0.5-diameter and 700-m-depth scenario, which relates only to the friction losses in the pipes, 0.24 MJ m<sup>-3</sup>, is

**Table 3** Primary production per hectare per year for chosen terrestrial and marine crops grown in deep sea water (for “artificial upwelling” 1 year = 330-day production)

Type of crop	Crop yield in protein (kg)	Crop yield (kg DW)	ExROI	Reference
Alfalfa (highest protein production)	710	6451	0.24	[40]
Corn silage (highest crop yield)	393	30,200 <sup>a</sup>	0.23	[40]
Cassava (lowest fossil energy input)	58	5824	0.0008	[40]
Artificial upwelling cultivated phytoplankton (optimum) <sup>b</sup>	23,063	39,764	0.31	[18]
Artificial upwelling cultivated <i>Ulva</i> sp. (scenario 11) <sup>c</sup>	590–1179	13,434–26,880	0.0054	Current study

<sup>a</sup> Fresh weight

<sup>b</sup> Optimum was decided upon according to cost/productivity considerations and relates to pool depth of 4.88 m

<sup>c</sup> Based on lab results projected to 0.625 or 1.25 m cultivation depth in the sea

**Table 4** Maximum pumping power per 10 ha for positive ExROI, according to the HIE

Depth (m)	250			350			700				
	1	2	3	1	2	3	1	2	3	5	10
Number of pipes	1	2	3	1	2	3	1	2	3	5	10
Current study pumping power (kW)	9.8E+02	2.0E+03	3.0E+03	1.4E+03	2.8E+03	4.1E+03	2.8E+03	5.5E+03	8.3E+03	1.4E+04	2.8E+04
Maximum pumping power for positive ExROI (kW)	4	9	14	10	21	25	12	38	35	89	149

equivalent to 21% of the maximum generated power in the EMS summer. Previous works have calculated a pumping cost of 6.5% of the power generation, suggesting results would be better in larger systems [18]. In general, larger-scale application may be of benefit, as the OTEC technology is expected to prove economic viability only in very large scales, applying larger diameters with lower losses [46].

### Local Israeli Geography

Productivity and energetic efficiency are highly dependent on the local geography of the upwelling site. By examining the local bathymetry, depths, yields, and energetic performances can be casted into the geographic context of the Israeli EEZ, thus enabling to designate specific locations as potential upwelling sites. The Israeli EEZ bathymetry is characterized by a continental shelf which measures a 2° slope in the south and about 8.5° slope in the north [47]. The steeper sea floor slopes in the North (Table 5) may be advantageous as it enables to locate the artificial upwelling sites closer to the shore, thus decreasing energetic requirements of transportation [9].

### Future Perspectives and Limitations

Finally, we believe that this work offers a path in which the vision of harnessing DSW nutrients for offshore macroalgae cultivation can advance from theory to real-world implementation. Our work emphasizes the importance of developing self-sufficient offshore power supply technologies as a preliminary step for artificial upwelling-based cultivation projects. Notwithstanding, the presented analysis is limited in its ability to represent exact DSW properties and real offshore conditions, including water exchange, flow, and dilution [20], as well as dynamic changes in nutrient concentrations [48]. Another limitation is the lack of data regarding the initial

**Table 5** Distance from the shore for each relevant sea depth, in four locations along the Israeli coast [47]

Depth (m)	250	350	700
Distance from shore (km)			
North (Atlit)	11	12	15
Caesarea	9	11	21
Center (Tel Aviv)	20	24	32
South (Ashkelon)	25	28	35

biomass composition. Ideally, this analysis should serve as a first step before following field experiments.

### Conclusions

We present an assessment of N supply for an offshore *Ulva* sp. cultivation project in the EMS, using DSW pumping. Based on laboratory cultivation experiments and upscaling simulations, measured RGRs of 6.3–7.4% were projected to the potential production of 8.5–17.1 ton dry *Ulva* sp. biomass, including 373–751 kg of protein and 742–1484 kg of starch within 21 cultivation days in an area of 10 ha, in the energetic cost of 4323–8656 MWh. These values offer high productivity but low energetic efficiency, compared to terrestrial crops. At last, we conclude that the energetic performance and the overall viability of this project will significantly increase once offshore self-sufficient power sources will be developed.

**Acknowledgments** The authors thank Mr. Jan Peene and Prof. Klaas Timmermans from NIOZ, Yerseke for assistance in nutrient measurement in ASW; Arthur Robin and Dr. Meghanath Prabhu for assistance in protein and starch measurements; and Yiftach Golov for assistance in statistical analysis.

**Funding Information** The Israel Ministry of Energy and Israel Ministry of Science and Technology, TAU Institute for Innovation in Transportation, and TAU Gordon Center for Energy provided funding. HT received funding from Boris Mints Institute and Tel-Aviv University Center for Renewable Energy. MZ received funding from the Manna Center Program for Food Safety and Security.

### Compliance with Ethical Standards

**Competing Interests** The authors declare that they have no conflict of interest.

### References

- Aitken D, Bulboa C, Godoy-Faundez A, Turrion-Gomez JL, Antizar-Ladislao B (2014) Life cycle assessment of macroalgae cultivation and processing for biofuel production. *J Clean Prod* 75: 45–56. <https://doi.org/10.1016/J.CLEPRO.2014.03.080>
- Postma PR, Cerezo-Chinarro O, Akkerman RJ, Olivier G, Wijffels RH, Brandenburg WA, Eppink MHM (2017) Biorefinery of the macroalgae *Ulva lactuca*: extraction of proteins and carbohydrates

- by mild disintegration. *J Appl Phycol* 30:1–13. <https://doi.org/10.1007/s10811-017-1319-8>
3. Balina K, Romagnoli F, Blumberga D (2017) Seaweed biorefinery concept for sustainable use of marine resources. *Energy Procedia* 128:504–511. <https://doi.org/10.1016/J.EGYPRO.2017.09.06>
  4. Cole A, Dinburg Y, Haynes BS, Yaya H, Herskowitz M, Jazrawi C, Landau M, Liang X, Magnusson M, Maschmeyer T, Masters AF, Meiri N, Neveux N, de Nys R, Paul N, Rabaev M, Vidruk-Nehemya R, Yuen AKL (2016) From macroalgae to liquid fuel via waste-water remediation, hydrothermal upgrading, carbon dioxide hydrogenation and hydrotreating. *Energy Environ Sci* 9:1828–1840. <https://doi.org/10.1039/c6ee00414h>
  5. Buschmann AH, Camus C, Infante J, Neori A, Israel Á, Hernández-González MC, Pereda SV, Gomez-Pinchetti JL, Golberg A, Tadmor-Shalev N, Critchley AT (2017) Seaweed production: overview of the global state of exploitation, farming and emerging research activity. *Eur J Phycol* 52:391–406. <https://doi.org/10.1080/09670262.2017.1365175>
  6. Fernand F, Israel A, Skjermo J, Wicharde T, Timmermans KR, Golberg A (2017) Offshore macroalgae biomass for bioenergy production: environmental aspects, technological achievements and challenges. *Renew Sust Energ Rev* 75:35–45. <https://doi.org/10.1016/J.RSER.2016.10.046>
  7. Segheta M, Hou X, Bastianoni S, Bjerrec A-B, Thomse M (2016) Life cycle assessment of macroalgal biorefinery for the production of ethanol, proteins and fertilizers – a step towards a regenerative bioeconomy. *J Clean Prod* 137:1158–1169. <https://doi.org/10.1016/j.jclepro.2016.07.195>
  8. Golberg A, Liberzon A (2015) Modeling of smart mixing regimes to improve marine biorefinery productivity and energy efficiency. *Algal Res* 11:28–32. <https://doi.org/10.1016/J.ALGAL.2015.05.021>
  9. Lehahn Y, Ingle KN, Golberg A (2016) Global potential of offshore and shallow waters macroalgal biorefineries to provide for food, chemicals and energy: feasibility and sustainability. <https://doi.org/10.1016/j.algal.2016.03.031>
  10. Korzen L, Pulidindi IN, Israel A, Abelson A, Gedanken A (2015) Marine integrated culture of carbohydrate rich *Ulva rigida* for enhanced production of bioethanol. *RSC Adv* 5:59251–59256. <https://doi.org/10.1039/C5RA09037G>
  11. Harrison, PJ., Hurd CL (2001) Nutrient physiology of seaweeds: application of concepts to aquaculture. *Cah de biol Mar*, 42(1-2), 71-82
  12. Markou G, Vandamme D, Muylaert K (2014) Microalgal and cyanobacterial cultivation: the supply of nutrients. *Water Res* 65: 186–202. <https://doi.org/10.1016/j.watres.2014.07.025>
  13. Trent J, Embaye T, Buckwalter P, Richardson T-M, Kagawa H, Reinsch S, Martis M (2010) Offshore membrane enclosures for growing algae (omega): a system for biofuel production, wastewater treatment, and CO<sub>2</sub> sequestration
  14. Troell M, Joyce A, Chopin T, Neori A, Buschmann AH, Fangh J-G (2009) Ecological engineering in aquaculture — potential for integrated multi-trophic aquaculture (IMTA) in marine offshore systems. *Aquaculture* 297:1–9. <https://doi.org/10.1016/J.AQUACULTURE.2009.09.010>
  15. Roesijadi G, Copping AE, Huesemann MH, Forster J, Benemann JR (2008) Techno-economic feasibility analysis of offshore seaweed farming for bioenergy and biobased products. Independent research and development report IR# PNWD-3931, Battelle Pacific Northwest Division, 115.
  16. YiWen P, Wei F, DaHai Z, Chen JW, Huang HC, Liu SX, Jiang ZP, Di YN, Tong MM (2016) Research progress in artificial upwelling and its potential environmental effects. *Sci China Earth Sci* 59:236–248. <https://doi.org/10.1007/s11430-015-5195-2>
  17. Zhang D, Fan W, Yang J, Yiwen P, Ying C, Haocai H, Jiawang C (2016) Reviews of power supply and environmental energy conversions for artificial upwelling. *Renew Sust Energ Rev* 56: 659–668. <https://doi.org/10.1016/J.RSER.2015.11.041>
  18. Roels OA, Laurence S, van Hemelryck L (1979) The utilization of cold, nutrient-rich deep ocean water for energy and mariculture. *Ocean Manag* 5(3), 199-210.
  19. Fan W, Chen J, Pan Y, Haocai H, Chen-Tung CA, Ying C (2013) Experimental study on the performance of an air-lift pump for artificial upwelling. *Ocean Eng* 59:47–57. <https://doi.org/10.1016/J.OCEANENG.2012.11.014>
  20. Williamson N, Komiya A, Maruyama S, Behnia M, Behniaet M (2009) Nutrient transport from an artificial upwelling of deep sea water. *J Oceanogr* 65:349–359
  21. Kress N, Herut B (2001) Spatial and seasonal evolution of dissolved oxygen and nutrients in the Southern Levantine Basin (Eastern Mediterranean Sea): chemical characterization of the water masses and inferences on the N:P ratios. *Deep Sea Res Part I Oceanogr Res Pap* 48:2347–2372. [https://doi.org/10.1016/S0967-0637\(01\)00022-X](https://doi.org/10.1016/S0967-0637(01)00022-X)
  22. Carl C, de Nys R, Paul NA (2014) The seeding and cultivation of a tropical species of filamentous *Ulva* for algal biomass production. *PLoS one* 9(6):e98700
  23. Chemodanov A, Robin A, Golberg A (2017) Design of marine macroalgae photobioreactor integrated into building to support seagriculture for biorefinery and bioeconomy. *Bioresour Technol* 241:1084–1093
  24. Parker HS (1981) Influence of relative water motion on the growth, ammonium uptake and carbon and nitrogen composition of *Ulva lactuca* (Chlorophyta). *Mar Biol* 63(3):309–318
  25. Steffensen DA (1976) The effect of nutrient enrichment and temperature on the growth in culture of *Ulva lactuca* L. *Aquat Bot* 2: 337–351
  26. Li H, Zhang Y, Han X, Shi X, Rivkin RB, Legendre L (2016) Growth responses of *Ulva prolifera* to inorganic and organic nutrients: implications for macroalgal blooms in the southern Yellow Sea, China. *Sci Rep* 6:26498. <https://doi.org/10.1038/srep26498>
  27. Reidenbach LB, Fernandez PA, Leal PP, Noisette F, McGraw CM, Revill AT, Hurd CL, Kübler JE (2017) Growth, ammonium metabolism, and photosynthetic properties of *Ulva australis* (Chlorophyta) under decreasing pH and ammonium enrichment. *PLoS One* 12:e0188389. <https://doi.org/10.1371/journal.pone.0188389>
  28. Luo MB, Liu F, Xu ZL (2012) Growth and nutrient uptake capacity of two co-occurring species, *Ulva prolifera* and *Ulva linza*. *Aquat Bot* 100:18–24. <https://doi.org/10.1016/J.AQUABOT.2012.03.006>
  29. de Casabianca M-L, Barthelemy N, Serrano O, Sfriso A (2002) Growth rate of *Ulva rigida* in different Mediterranean eutrophicated sites. *Bioresour Technol* 82:27–31. [https://doi.org/10.1016/S0960-8524\(01\)00155-9](https://doi.org/10.1016/S0960-8524(01)00155-9)
  30. Lowry OH, Rosebrough NJ, Farr AL, Randall RJ (1951) Protein measurement with the Folin phenol reagent. *J Biol Chem*
  31. Barbarino E, Lourenço SO (2005) An evaluation of methods for extraction and quantification of protein from marine macro- and microalgae. *J Appl Phycol* 17:447–460. <https://doi.org/10.1007/s10811-005-1641-4>
  32. Zollmann M, Traugott H, Chemodanov A, Liberzon A, Golberg A (2018) Exergy efficiency of solar energy conversion to biomass of green macroalgae *Ulva* (Chlorophyta) in the photobioreactor. *Energy Convers Manag* 167:125–133. <https://doi.org/10.1016/J.ENCONMAN.2018.04.090>
  33. Characteristics of Photosynthetic Active Radiation (PAR) Through statistical analysis at Lamaca, Cyprus
  34. Jacovides CP, Tymvios FS, Asimakopoulos DN, Theofilou KM, Pashiardes S (2003) Global photosynthetically active radiation and its relationship with global solar radiation in the Eastern Mediterranean basin. *Theor Appl Climatol* 74:227–233. <https://doi.org/10.1007/s00704-002-0685-5>

35. Da Rocha HSD, Marques PA, De Camargo APD, Frizzone JA, Saretta E (2017) Internal surface roughness of plastic pipes for irrigation. *Revista Brasileira de Engenharia Agrícola e Ambiental*, 21(3), 143–149. <https://doi.org/10.1590/1807-1929/agriambi.v21n3p143-149>
36. Korzen L, Abelson A, Israel A (2016) Growth, protein and carbohydrate contents in *Ulva rigida* and *Gracilaria bursa-pastoris* integrated with an offshore fish farm. *J Appl Phycol* 28:1835–1845. <https://doi.org/10.1007/s10811-015-0691-5>
37. Rosenberg, C., Ramus J (1982) Ecological growth strategies in the seaweeds *Gracilaria foliifera* (Rhodophyceae) and *Ulva* sp. (Chlorophyceae): soluble nitrogen and reserve carbohydrates. *Mar Biol*, 66(3): 251–259.
38. Hanisak MD (1979) Nitrogen limitation of *Codium fragile* ssp. *tomentosoides* as determined by tissue analysis. *Mar Biol* 50:333–337
39. Lourenco SO, Barbarino E, De-Paula JC et al (2002) Amino acid composition, protein content and calculation of nitrogen-to-protein conversion factors for 19 tropical seaweeds. *Phycol Res* 50:233–241. <https://doi.org/10.1046/j.1440-1835.2002.00278.x>
40. Pimentel D, Dritschilo W, Krummel J, Kutzman J (1975) Energy and land constraints in food protein production. *Science* (80-) 190: 754–761. <https://doi.org/10.1126/science.184.4134.307>
41. Kim S, Dale BE (2004) Global potential bioethanol production from wasted crops and crop residues. *Biomass Bioenergy* 26: 361–375. <https://doi.org/10.1016/J.BIOMBIOE.2003.08.002>
42. Ziska LH, Runion GB, Tomecek M, Prior SA, Torbet HA, Sicheira R (2009) An evaluation of cassava, sweet potato and field corn as potential carbohydrate sources for bioethanol production in Alabama and Maryland. *Biomass Bioenergy* 33:1503–1508. <https://doi.org/10.1016/J.BIOMBIOE.2009.07.014>
43. Aure J, Strand Ø, Erga S, Strohmeier T (2007) Primary production enhancement by artificial upwelling in a western Norwegian fjord. *Mar Ecol Prog Ser* 352:39–52. <https://doi.org/10.3354/meps07139>
44. Liu CCK, Jin Q (1995) Artificial upwelling in regular and random waves
45. White A, Björkman K, Grabowski E, Letelier R, Poulos S, Watkins B, Karl D (2010) An Open Ocean trial of controlled upwelling using wave pump technology. *J Atmos Ocean Technol* 27:385–396. <https://doi.org/10.1175/2009JTECHO679.1>
46. Meyer L, Cooper D, Varley R (2011) Are we there yet? In: OCEANS'11 MTS/IEEE KONA, Waikoloa, HI, pp. 1–6. doi: 10.23919/OCEANS.2011.6107297
47. Emery K, Bentor Y (1960) The continental shelf of Israel
48. Ren JS, Barr NG, Scheuer K, Schiel DR, Zeldis J (2014) A dynamic growth model of macroalgae: application in an estuary recovering from treated wastewater and earthquake-driven eutrophication. *Estuar Coast Shelf Sci* 148:59–69. <https://doi.org/10.1016/J.ECSS.2014.06.014>

**Publisher's Note** Springer Nature remains neutral with regard to jurisdictional claims in published maps and institutional affiliations.